REPORT DOCUMENTATION PAGE

Form Approved OMB NO. 0704-0188

1. REPORT DATE (DD-MM-YYYY)	2. REPORT TYPE	3. DATES COVERED (From - To)
22-06-2014	Final Report	1-Sep-2013 - 31-May-2014

4. TITLE AND SUBTITLE
Advanced Antenna Measurement Processing

5a. CONTRACT NUMBER
W911NF-13-1-0369

5b. GRANT NUMBER

5c. PROGRAM ELEMENT NUMBER
611102

6. AUTHORS
Ronald J. Pogorzelski, Sembiam R. Rengarajan

5d. PROJECT NUMBER

5e. TASK NUMBER

5f. WORK UNIT NUMBER

7. PERFORMING ORGANIZATION NAMES AND ADDRESSES
California State University - Northridge
18111 Nordhoff Street

Northridge, CA 91330 -8232

8. PERFORMING ORGANIZATION REPORT NUMBER

9. SPONSORING/MONITORING AGENCY NAME(S) AND ADDRESS (ES)
U.S. Army Research Office
P.O. Box 12211
Research Triangle Park, NC 27709-2211

10. SPONSOR/MONITOR'S ACRONYM(S)
ARO

11. SPONSOR/MONITOR'S REPORT NUMBER(S)
64550-EL-II.1

12. DISTRIBUTION AVAILIBILITY STATEMENT
Approved for Public Release; Distribution Unlimited

13. SUPPLEMENTARY NOTES
The views, opinions and/or findings contained in this report are those of the author(s) and should not contrued as an official Department of the Army position, policy or decision, unless so designated by other documentation.

14. ABSTRACT
This research project is focused on the advancement of methods of post measurement processing of antenna pattern measurements to enhance their utility in assessment of antenna performance. Three specific techniques are treated; planar near-field extrapolation, planar near-field extended probe calibration, and the “Super Iso-filter” for separation of the radiation field into components originating from specified regions of the radiating structure. We show that planar near field measurement maybe extrapolated beyond the scan plane sampling region to provide wider angle far field results than otherwise obtainable. We also show that a calibration measurement in planar near

15. SUBJECT TERMS
Antennas, Nearfield Measurement, Post-Measurement Computer Processing

16. SECURITY CLASSIFICATION OF:			17. LIMITATION OF ABSTRACT	15. NUMBER OF PAGES	19a. NAME OF RESPONSIBLE PERSON
a. REPORT	b. ABSTRACT	c. THIS PAGE			Ronald Pogorzelski
UU	UU	UU	UU		19b. TELEPHONE NUMBER 818-677-2190

Report Title

Advanced Antenna Measurement Processing

ABSTRACT

This research project is focused on the advancement of methods of post measurement processing of antenna pattern measurements to enhance their utility in assessment of antenna performance. Three specific techniques are treated; planar near-field extrapolation, planar near-field extended probe calibration, and the "Super Iso-filter" for separation of the radiation field into components originating from specified regions of the radiating structure. We show that planar near field measurement maybe extrapolated beyond the scan plane sampling region to provide wider angle far field results than otherwise obtainable. We also show that a calibration measurement in planar near field scanning can be used to remove artifacts arising from multipath effects on the measurement range. Finally, we demonstrate that the iterative processing embodied in the Super Iso-filter algorithm provides an effective and rigorously correct means of separating the radiation from two separate antennas using only data measured for both antennas radiating simultaneously. The three techniques treated here provide convenient and useful tools to the antenna engineer in designing and assessing the performance of antennas for practical use.

Enter List of papers submitted or published that acknowledge ARO support from the start of the project to the date of this printing. List the papers, including journal references, in the following categories:

(a) Papers published in peer-reviewed journals (N/A for none)

Received Paper

TOTAL:

Number of Papers published in peer-reviewed journals:

(b) Papers published in non-peer-reviewed journals (N/A for none)

Received Paper

TOTAL:

Number of Papers published in non peer-reviewed journals:

(c) Presentations

Number of Presentations: 0.00

Non Peer-Reviewed Conference Proceeding publications (other than abstracts):

Received Paper

TOTAL:

Number of Non Peer-Reviewed Conference Proceeding publications (other than abstracts):

Peer-Reviewed Conference Proceeding publications (other than abstracts):

Received Paper

TOTAL:

Number of Peer-Reviewed Conference Proceeding publications (other than abstracts):

(d) Manuscripts

Received Paper

TOTAL:

Number of Manuscripts:

Books

Received Book

TOTAL:

Received	Book Chapter

TOTAL:

Patents Submitted

Patents Awarded

Awards

Graduate Students

NAME	PERCENT_SUPPORTED
FTE Equivalent:	
Total Number:	

Names of Post Doctorates

NAME	PERCENT_SUPPORTED
FTE Equivalent:	
Total Number:	

Names of Faculty Supported

NAME	PERCENT_SUPPORTED	National Academy Member
Ronald J. Pogorzelski	1.00	
Sembiam R. Rengarajan	0.06	
FTE Equivalent:	**1.06**	
Total Number:	**2**	

Names of Under Graduate students supported

NAME	PERCENT_SUPPORTED
FTE Equivalent:	
Total Number:	

Student Metrics

This section only applies to graduating undergraduates supported by this agreement in this reporting period

The number of undergraduates funded by this agreement who graduated during this period: 0.00

The number of undergraduates funded by this agreement who graduated during this period with a degree in science, mathematics, engineering, or technology fields:..... 0.00

The number of undergraduates funded by your agreement who graduated during this period and will continue to pursue a graduate or Ph.D. degree in science, mathematics, engineering, or technology fields:..... 0.00

Number of graduating undergraduates who achieved a 3.5 GPA to 4.0 (4.0 max scale):..... 0.00

Number of graduating undergraduates funded by a DoD funded Center of Excellence grant for Education, Research and Engineering:..... 0.00

The number of undergraduates funded by your agreement who graduated during this period and intend to work for the Department of Defense 0.00

The number of undergraduates funded by your agreement who graduated during this period and will receive scholarships or fellowships for further studies in science, mathematics, engineering or technology fields:..... 0.00

Names of Personnel receiving masters degrees

NAME

Total Number:

Names of personnel receiving PHDs

NAME

Total Number:

Names of other research staff

NAME PERCENT_SUPPORTED

FTE Equivalent:

Total Number:

Sub Contractors (DD882)

Inventions (DD882)

Scientific Progress

Executive Summary (Full report attached as pdf.)

The research described here advances the development of three post measurement processing techniques applicable to antenna pattern data. The advancements were achieved through experimental demonstration of each technique via suitable measurements and subsequent computation. The results provide evidence that the three techniques enable antenna performance assessment in greater detail and with greater fidelity than previously attainable.

The first technique is a means of extrapolating the data sampled over a near-field plane to an area greater than that sampled. The advantage attained is an expansion of the accessible angular range in the far field for a given measurement plane sampling area. Ultimately, we hope to achieve extrapolation resulting in full hemispherical far zone coverage but this has proved elusive to date. Nevertheless, we have been able to develop a new algorithm that does not suffer from the disturbing divergence behavior noted in the traditional Gerchberg-Papoulis approach to this problem. What is still needed is a means of predicting the maximum far field angular range achievable by such extrapolation in a given situation where the far zone pattern is unknown.

The second advance is the application of the so-called EPIC algorithm, originally developed for spherical near-field measurements, to planar scanning. The algorithm is designed to eliminate multipath effects. One measures a calibration antenna for which the far zone pattern is known and uses the results to “calibrate out” the multipath effects. Essentially, one views as the “extended probe” the actual probe plus the scattering objects causing the multipath and performs a probe correction for this extended probe. This, of course, requires that the probe remain fixed while the antenna under test is scanned past it. We simulated the multipath by using a second probe in addition to the primary one. The demonstration showed effective removal of the multipath effects over a large portion of the pattern limited by the dynamic range of the system. We further demonstrated this technique in an actual, rather than simulated, multipath environment. There remain some theoretical issues concerning the equivalence principle in this context that should be studied as these may limit the location of scatterers that can be calibrated out.

Thirdly, we demonstrated the so-called Super Iso-filter which is an iterative technique for rigorously separating the radiation from individual parts of an antenna structure. We did this by measuring a combination of a standard gain horn and a four element circularly polarized patch array radiating simultaneously. By processing the resulting data in an iterative fashion we separated the radiation into two parts, that radiated by the horn and that radiated by the patch array. We note that each part includes the currents induced on the given antenna by radiation from the other; i.e., mutual coupling. We further point out that there is no other known way to experimentally obtain these results because separate measurement of the antennas does not account for mutual coupling and separate excitation of the antennas does not separate the radiation from the scattering.

Further work is required to explore the limits on antenna separation for effective field decomposition as well as the convergence properties of the iteration. Applicability to more than two radiators is also fertile ground for investigation and development.

Overall, we have achieved significant progress but have by no means exhausted these avenues of investigation. Several issues should be investigated in more detail as mentioned above. Moreover, demonstrations in more general geometries would lend credence to the wide applicability of these methods and related techniques yet to be developed.

Technology Transfer

Advanced Antenna Measurement Processing

Dr. Ronald J. Pogorzelski, PI
Professor Sembiam R. Rengarajan, Co-I

California State University, Northridge
Project No. 40054464

a research and development project for the
United States Army Research Office

Final Report
June 18, 2014

Contact:
Dr. Ronald J. Pogorzelski
Mail Stop
Dept. of Electrical and Computer Engineering
California State University, Northridge
18111 Nordhoff Street
Northridge, CA 91330-8346
(818)377-6585 FAX: (818)377-7062
Ronald.Pogorzelski@csun.edu

Table of Contents

Advanced Antenna Measurement Processing

Dr. Ronald J. Pogorzelski, PI
Professor Sembiam R. Rengarajan, Co-I

CSUN Project No. 40054464

Executive Summary

The research described here advances the development of three post measurement processing techniques applicable to antenna pattern data. The advancements were achieved through experimental demonstration of each technique via suitable measurements and subsequent computation. The results provide evidence that the three techniques enable antenna performance assessment in greater detail and with greater fidelity than previously attainable.

The first technique is a means of extrapolating the data sampled over a near-field plane to an area greater than that sampled. The advantage attained is an expansion of the accessible angular range in the far field for a given measurement plane sampling area. Ultimately, we hope to achieve extrapolation resulting in full hemispherical far zone coverage but this has proved elusive to date. Nevertheless, we have been able to develop a new algorithm that does not suffer from the disturbing divergence behavior noted in the traditional Gerchberg-Papoulis approach to this problem. What is still needed is a means of predicting the maximum far field angular range achievable by such extrapolation in a given situation where the far zone pattern is unknown.

The second advance is the application of the so-called EPIC algorithm, originally developed for spherical near-field measurements, to planar scanning. The algorithm is designed to eliminate multipath effects. One measures a calibration antenna for which the far zone pattern is known and uses the results to "calibrate out" the multipath effects. Essentially, one views as the "extended probe" the actual probe plus the scattering objects causing the multipath and performs a probe correction for this extended probe. This, of course, requires that the probe remain fixed while the antenna under test is scanned past it. We simulated the multipath by using a second probe in addition to the primary one. The demonstration showed effective removal of the multipath effects over a large portion of the pattern limited by the dynamic range of the system. We further demonstrated this technique in an actual, rather than simulated, multipath environment. There remain some theoretical issues concerning the equivalence principle in this context that should be studied as these may limit the location of scatterers that can be calibrated out.

Thirdly, we demonstrated the so-called Super Iso-filter which is an iterative technique for rigorously separating the radiation from individual parts of an antenna structure. We did this by measuring a combination of a standard gain horn and a four element circularly polarized patch array radiating simultaneously. By processing the resulting data in an iterative fashion we separated the radiation into two parts, that radiated by the horn and that radiated by the patch array. We note that each part includes the currents induced on the given antenna by radiation from the other; i.e., mutual coupling. We further point out that there is no other known way to experimentally obtain these results because separate measurement of the antennas does not account for mutual coupling and separate excitation of the antennas does not separate the radiation from the scattering. Further work is required to explore the limits on antenna separation for effective field decomposition as well as the convergence properties of the iteration. Applicability to more than two radiators is also fertile ground for investigation and development.

Overall, we have achieved significant progress but have by no means exhausted these avenues of investigation. Several issues should be investigated in more detail as mentioned above. Moreover, demonstrations in more general geometries would lend credence to the wide applicability of these methods and related techniques yet to be developed.

Advanced Antenna Measurement Processing

Dr. Ronald J. Pogorzelski, PI
Professor Sembiam R. Rengarajan, Co-I

CSUN Project No. 40054464

Final Report

Abstract

This research project is focused on the advancement of methods of post measurement processing of antenna pattern measurements to enhance their utility in assessment of antenna performance. Three specific techniques are treated; planar near-field extrapolation, planar near-field extended probe calibration, and the "Super Iso-filter" for separation of the radiation field into components originating from specified regions of the radiating structure. We show that planar near field measurement maybe extrapolated beyond the scan plane sampling region to provide wider angle far field results than otherwise obtainable. We also show that a calibration measurement in planar near field scanning can be used to remove artifacts arising from multipath effects on the measurement range. Finally, we demonstrate that the iterative processing embodied in the Super Iso-filter algorithm provides an effective and rigorously correct means of separating the radiation from two separate antennas using only data measured for both antennas radiating simultaneously. The three techniques treated here provide convenient and useful tools to the antenna engineer in designing and assessing the performance of antennas for practical use.

Introduction

Because communication and remote sensing are central to the activities of the modern warfighter, antenna engineering as a discipline is crucial to the mission of the U. S. Army. It is therefore an important component of advanced educational programs that train engineers for employment in the defense industry and elsewhere. Antenna engineering embodies the design of effective antennas via electromagnetic theory and practice and testing for verification of the performance of the resulting antennas. Antenna testing includes measurement of the terminal characteristics of the antenna such as input impedance and return loss as well as the radiation characteristics such as directivity and sidelobe level; in essence, the antenna radiation pattern.

Antenna pattern measurements have historically been conducted by placing a probe in the far zone of the antenna and rotating the antenna so as to sample a so-called pattern cut. The pattern cut is usually taken at a fixed roll angle although specialized sampling has on occasion been used

to produce roll cuts or spinning linear polarization plots. Modern antenna measurements are often done in the near field of the antenna with a subsequent mathematical transformation to the far zone. The near field is sampled either by moving the antenna or by moving the probe or by a combination of both. The sampling typically is done on a canonical surface, planar, cylindrical, or spherical to facilitate the mathematics but in principle it can be done on any surface.

Once mathematical transformation is introduced as part of the measurement process, one may, without significant complication, utilize a number of post measurement processing techniques to enhance the extent and quality of the results or to reveal characteristics of the data not readily discernable without such processing. The present research is directed at further development of several such post measurement processing methods providing attractive antenna assessment capabilities of interest to antenna engineers.

Objectives

The project as proposed embodied two specific objectives, experimental demonstration of the "Super Iso-filter" concept [1] and application of the principles of the "EPIC" technique [2] [3], originally developed for spherical measurement systems, to planar scanning. However, the desirability of a third objective came to light as the work on the EPIC objective progressed. This third objective is development of a technique for extrapolation of a planar scan to wider angles than are accessible via standard processing. This development addresses a limitation inherent in all planar near field scanning systems. That is, the range of far field angles over which far field data can be computed via the near field to far field transformation is limited by the extent of the scan area in the near field. Rules of thumb for estimating the limiting angles are provided by the manufacturers of the scanning equipment and these imply that it is difficult to exceed 60 to 70 degrees from the antenna boresight with reasonable scan plane extent. Ideally, it would be desirable to obtain far field data out to 90 degrees from boresight because it would then be possible to obtain results over the entire far zone sphere from two near field scans, one for the front hemisphere and one for the back hemisphere. We believe that achievement of this third objective would represent a significant enhancement of the planar EPIC technique investigated in this research activity.

It is important to recognize, however, that the extent of the measurement plane is not the only factor that limits the angular range of the far zone results. An additional limitation arises because of the attainable accuracy of the measurements which translates into the available dynamic range. For example, if the error in the electric field measurement is one part in a thousand (0.1%) then the error will appear as a 6 dB ripple 60 dB below the maximum measured value, which ideally would be just short of receiver saturation. This error may also be seen as a 0.83 dB ripple at the -40 dB level or a 1 dB ripple at the -41.73 dB level. If we arbitrarily select 1 dB ripple to be the maximum acceptable error, we describe this as a measurement with a 41.73 dB available dynamic range. Now, typically probe correction reduces the available dynamic range. As an example of this, consider a far field measurement carried out in the E-plane of an antenna using an open ended waveguide probe in a system with a 40 dB dynamic range. The far zone field of the probe drops about 16 dB from boresight to 90 degrees in azimuth. When the corresponding probe correction is applied (essentially dividing the measured far field by the

corresponding probe far field at each azimuth angle) the result will have an available dynamic range of only 24 dB (40 dB – 16 dB). Thus, the range of azimuth angles over which the result is accurate to 1 dB is limited to that over which the far zone antenna pattern lies within 24 dB of the maximum. This limit applies even if the measurement were done in the near field and subsequently transformed to the far field independent of the extent of the near field scan. The limit imposed by the extent of the scan may be more or less stringent than this limit. Ultimately, the limit of the angular range is the more stringent of the two.

Extrapolation in Planar Near-field Scanning

In planar near field scanning we use an NSI 5 by 5 foot planar scanner with an HP 8530A Receiver, an HP 83620A Synthesized Sweeper, and an HP 8511A Frequency Converter. The system was recently upgraded with a new Dell T3600 workstation running the NSI2000 Software Professional Version V4.9.018, June 10, 2013. We note that, except as otherwise noted, we export the raw measured data and use our own software for the near field to far field transformation. This software employs the Huygens approximation to relate the aperture electric and magnetic equivalent currents.

As outlined above, the ultimate objective is to obtain far field data over an entire sphere surrounding the antenna under test in a planar near field scanning geometry. Focusing first on the front hemisphere, this would at first glance seem to require scanning over a measurement plane of infinite extent. What is needed then is a means of extrapolating to the full hemisphere the results of a measurement of finite extent. This problem has been recently addressed by Martini, et al.[4] They define a region of the surface of the far zone sphere as the "reliable region." Within this region, the result of transformation of the measured data over a finite size scan plane is assumed to be accurate. Moreover, it is the far field of a radiating aperture of finite extent and is therefore band-limited in spatial frequency. Extrapolation of such a function may be achieved via the well-known Gerchberg-Papoulis (G-P) algorithm [5][6] and Martini, et al apply it to extrapolate the far zone field from the reliable region to the full hemisphere. However, their results exhibit a disturbing divergence after a number of iterations which they attribute at least in part to inaccuracy in estimating the far fields in the reliable region from data over a finite measurement plane. We have developed an alternative to the G-P algorithm that avoids this difficulty. [7]

The essence of the G-P algorithm is this. Beginning with a sample of a band limited function extending over a finite range, one obtains an estimate of its spectrum by Fourier transformation of this finite sample. Of course, the spectrum is no longer band limited due to the finite extent of the sample. Nevertheless, one truncates the spectrum to the known bandwidth and employs the inverse transform to obtain a new estimate of the original function. This new estimate now extends outside the range of the original sample. The key feature of the G-P algorithm is that at this point the new estimate of the original function is *replaced* with the original function over the original sample range while the portion outside this range is left as is. Then, the spectrum of the result is obtained via the Fourier transform and the process is repeated. In the work of Martini, et al., the limited range measured data over the scan plane is transformed to the far zone and the region near boresight is deemed "reliable." This "reliable" data is the finite range sample of a

band limited function. Its spectrum is obtained via Fourier transform and interpreted as the aperture distribution. This distribution is then truncated to the known aperture and its far field obtained via inverse Fourier transform. Per the G-P prescription, the data within the reliable region is replaced with the original field in that region and the process is repeated.

In contradistinction, our algorithm is as follows. We begin with the data measured over the measurement plane of finite extent and assume it to be "reliable." We then "zero-pad" to a larger region, obtain the plane wave spectrum of the padded function via Fourier transformation, and translate each plane wave to the aperture plane of the antenna under test. Summing the plane waves in the aperture plane via inverse Fourier transformation yields an estimate of the aperture distribution which has infinite extent. We then truncate this distribution to the known aperture and compute the corresponding plane wave spectrum via Fourier transformation. We translate each plane wave to the measurement plane and compute the field in that plane via inverse Fourier transformation. This new distribution is of infinite extent but, of course, we use a finite size transform corresponding to the zero-padded measured field. This new measurement plane field distribution extends to the entire range of the transform. In the spirit of the G-P algorithm, we replace this distribution with the original measured data within the original measurement range and leave the portion outside that range as is. The process is then repeated to convergence. Because this process uses directly measured values as the "reliable" data, it avoids the estimation error introduced in the "reliable" far zone data in the method of Martini, et al. The essential difference between our method and that of Martini, et al. then is that we iterate between the measurement plane and the aperture plane while they iterate between the far zone and the aperture plane. Thus, our method eliminates the need to first calculate the far fields in the "reliable region," a calculation that introduces error from the outset into data that is used repeatedly throughout the iteration. Note that, were the measurement to be done in the far zone, the two methods would become identical and embody the advantage that the "reliable" data is then, in both cases, directly measured rather than derived.

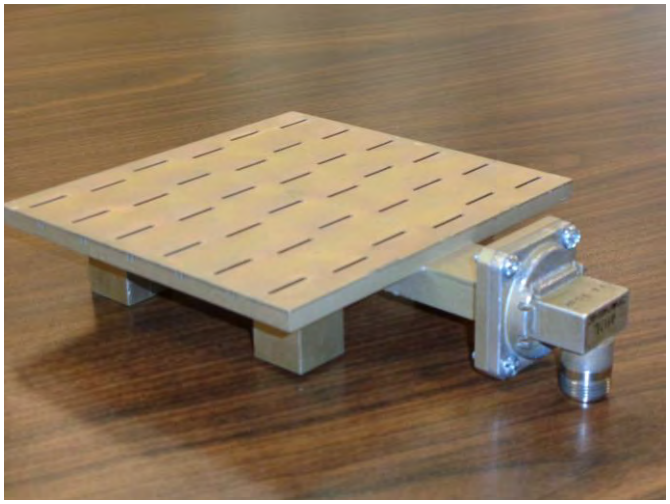

Figure 1. X-Band Slot Array.

As an example of the application of our method of extrapolation, we consider the six by six element 9.3 GHz slot array shown in Figure 1 and having a nominal directivity of 23 dB. This antenna was measured on an NSI Planar Near-field Scanner using a WR-90 open ended waveguide probe. The scan plane was 30 by 30 inches, sampled every quarter inch, and located 8.25 inches in front of the aperture. This geometry provides a far zone azimuth range from about -55 to +55 degrees. Figure 2 shows in dashed lines the H-plane data in the measurement plane and aperture plane as well as the resulting far zone radiation pattern without probe correction. Also shown in solid lines are the corresponding results after five iterations of truncating the aperture to 6.75 by 5.5 inches. (The E-plane truncation of 5.5 inches is based on the physical aperture dimension and has little impact on the H-plane calculations shown here. The H-plane truncation of 6.75 inches is based on the null locations in the aperture plane plot. Truncation in the nulls is presumed to cause minimal perturbation.) Note that the iteration has increased the azimuth limit from 55 degrees to 90 degrees. We choose to display the far zone pattern without probe correction so that the plot directly shows the dynamic range of the measurement. Had we displayed the probe corrected results, the dynamic range would have been reduced by the probe pattern excursion in dB.

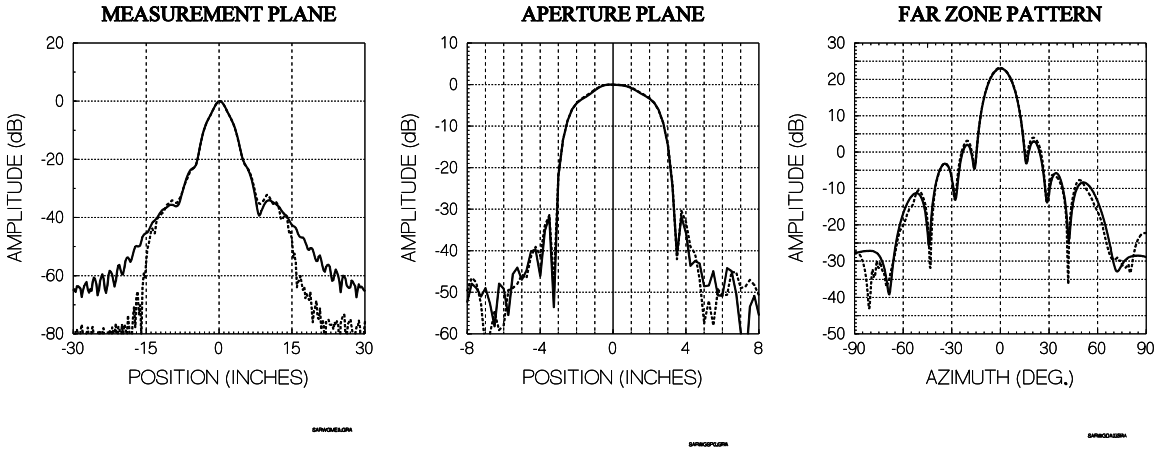

Figure 2. Distributions in the measurement plane, the aperture plane, and far zone before (dashed) and after (solid) five iterations without probe correction.

To further illustrate the extrapolation, we consider the case where only one quarter of the measurement plane data is used, half in each dimension. That is, the input is the data in a 15 inch square rather than the 30 inch one. This would give correct far field results out to only 27.5 degrees from normal according to the usual rule of thumb. The plots in Figure 3 bear this out where the solid lines are the result of iteration on the entire 30 inch data (dashed lines from Figure 2) and the dashed lines are the direct result of the 15 inch data with no iteration. Note that they agree only out to about 30 degrees.

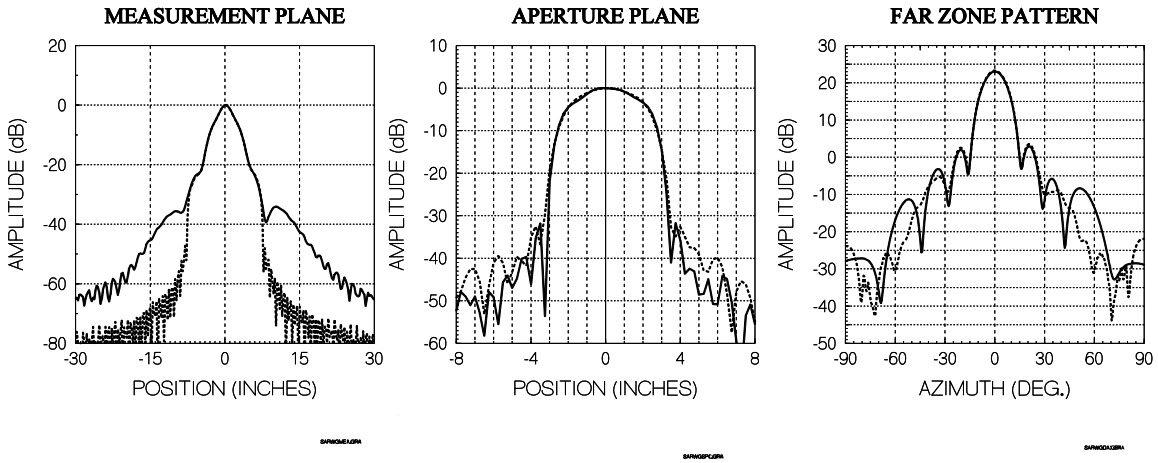

Figure 3. Distributions in the 15 inch measurement plane, the aperture plane, and far zone before iteration and without probe correction (dashed) compared with the result of iteration using the full measurement plane (solid).

Figure 4 shows the corresponding results where now the dashed curve is obtained after 100 iterations on the 15 inch data. It is evident that the iteration has expanded the valid azimuth region from ±30 degrees to ±45 degrees.

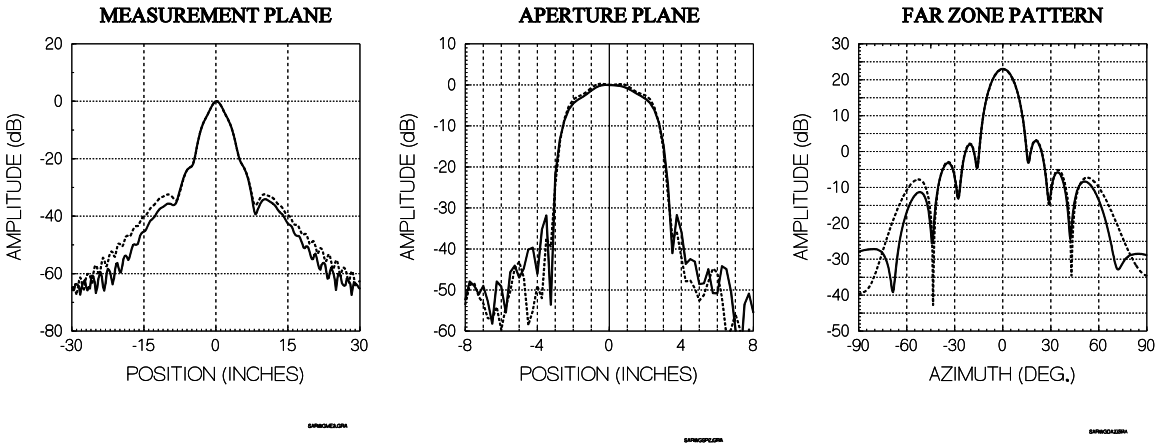

Figure 4. Distributions in the 15 inch measurement plane, aperture plane, and far field after 100 iterations and without probe correction (dashed) compared with the result of iteration using the full measurement plane (solid).

Generally we have found that truncating the aperture at a larger size requires more iterations for convergence but can lead to slightly better results. An example of this is shown in Figure 5 where we have increased the aperture size by one inch in the H-plane and employed 200 iterations thereby extending the far zone azimuth range to about ±50 degrees. Employing these parameters using the full 30 inches of input data essentially duplicates the results of Figure 2. In application, it will be desirable to provide an internal convergence determination based perhaps on the change from iteration to iteration so as to relieve the user of trial and error in this regard.

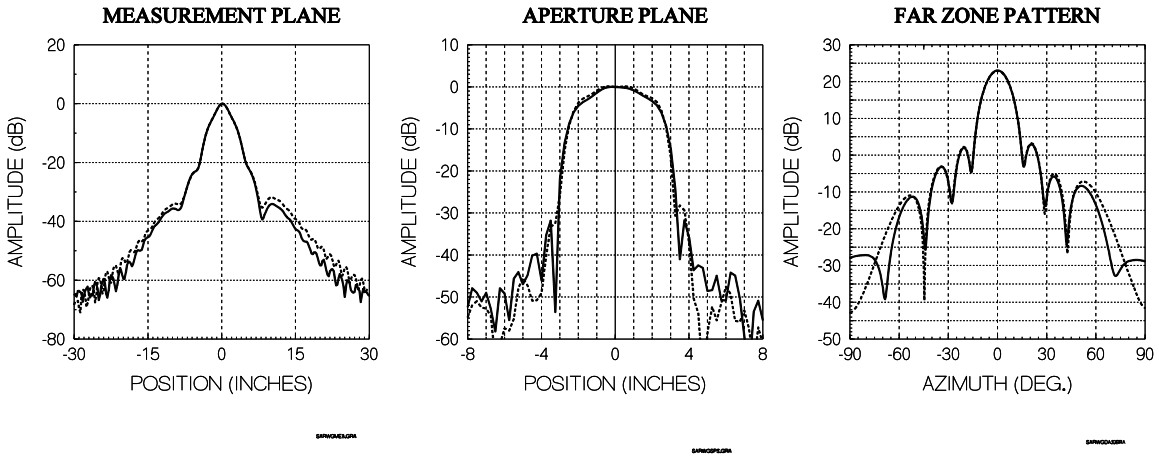

Figure 5. Distributions in the 15 inch measurement plane, aperture plane and far field after 200 iterations with enlarged aperture and without probe correction (dashed) compared with the result of iteration using the full measurement plane (solid).

Concerning the issue of aperture truncation, recognizing that the effective aperture is the convolution of the AUT aperture and the probe aperture leads one to truncate at $\pm(D_A+D_P)/2$ where D_A is the AUT aperture dimension and D_P is the probe aperture dimension in the plane in question, E or H. In the example above this would indicate truncation at ±3.3 inches in the H-plane and ±2.9 inches in the E-plane; i.e., a 5.8 by 6.6 inch rectangle. However, as seen in the aperture plane plots, the aperture distribution is not precisely zero outside the aperture which suggests that one should truncate at a slightly larger dimension as we have done in the H-plane in the examples.

Planar EPIC

The Extended Probe Instrument Calibration (EPIC) technique was reported recently as applied in spherical nearfield scanning.[2][3] In essence, the technique requires that one view the "extended probe" in nearfield measurement as consisting of the actual probe together with all stationary objects in the measurement chamber. Thus, in application of this technique, it is the antenna under test (AUT) that must move, while the probe remains stationary. The AUT consists of all objects that move with the antenna during the scan. One measures an antenna of known far field pattern and from that measurement infers the sensitivity of the extended probe to each spherical mode. This information is then used to correct the measurement of an unknown antenna for the measurement characteristics of the extended probe. Thus, EPIC is something of an extended probe correction. It was noted in the earlier work that the best calibration antenna is one with a low gain so an open ended waveguide was used. This preference carries over to the planar nearfield application as well.

While the planar EPIC technique is intended to remove from the measurement artifacts due to scatterers in the laboratory in which the planar scanner is located, these will typically be very small. In order to render the effects clearly visible and analyzable, we simulate a substantial artifact using a second probe. That is, any scatterer will provide a second path for a signal from

the AUT to the probe, much as if a second probe were placed at the location of the scatterer and its signal combined with that of the primary probe. Artifacts may be located anywhere in the front hemisphere of the AUT but the greater the lateral distance between the primary probe and the artifact the finer the sampling required to resolve the interference ripples in the pattern of the extended probe. For demonstration purposes, our extended probe consists of two horns fed by a 3 dB waveguide splitter as shown in Figure 6. One horn was selected as the primary probe and a small absorber plug was placed in the other horn to attenuate its signal thus preventing the undesirable occurrence of nulls in the pattern of the extended probe. (Of course, when using a standard open ended waveguide probe in the presence of small artifacts, it is highly unlikely that nulls would occur. One would expect in such typical cases that the artifacts would merely result in small ripples on the broad null free pattern of the primary probe.)

Figure 6. Extended probe.

In our demonstration the AUT is the 9.3 GHz slot array shown in Figure 1. The calibration antenna is chosen to be an open ended WR-90 waveguide. Following the EPIC prescription we first conduct a near field scan in which the extended probe is fixed and the calibration antenna is scanned in a 30 by 30 inch plane. Then transforming to the far zone we divide the pattern point by point by the known pattern of the calibration antenna (in this case the open ended waveguide). The result is the far zone pattern of the dual probe in the H-plane shown in Figure 7. Next, the calibration antenna is replaced by the AUT and a second scan is performed. The resulting far zone H-plane pattern is shown in Figure 8. Now, in this case, the EPIC algorithm merely consists of dividing the complex pattern of the second measurement by that of the first; that is, dividing the pattern of Figure 8 by that of Figure 7. The result is shown in Figure 9 as a solid curve. Also shown as a dashed curve is the probe corrected result of a direct measurement of the slot array using an open ended waveguide probe. This is essentially the probe corrected version of the dashed far zone pattern of Figure 2 (although it was obtained from a separate measurement). We obtained the pattern of the open ended waveguide calibration antenna by performing a planar scan of it using an essentially identical open ended waveguide probe and transforming the result to the far zone. Since this far zone pattern is the product of the patterns of the two open ended waveguides, we were able to obtain the pattern of one of them by merely taking the complex square root of the composite pattern. The result is shown in Figure 10.

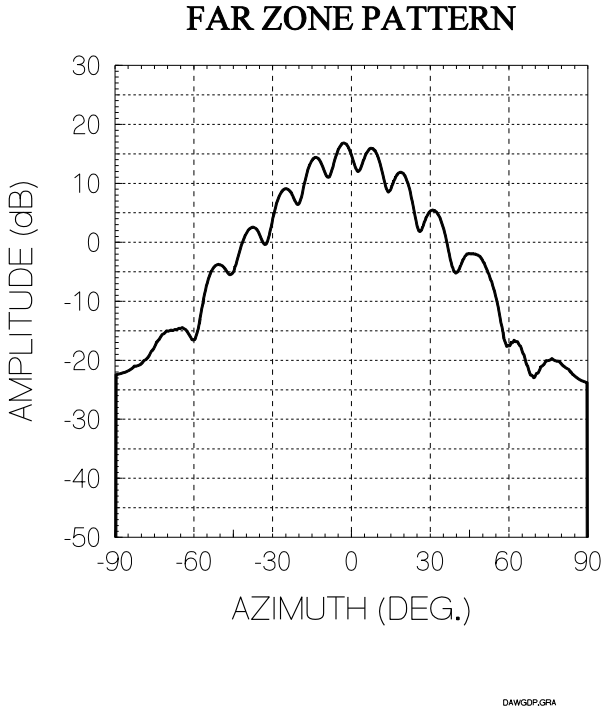

Figure 7. Far zone pattern of the dual probe obtained from measurement of the calibration antenna.

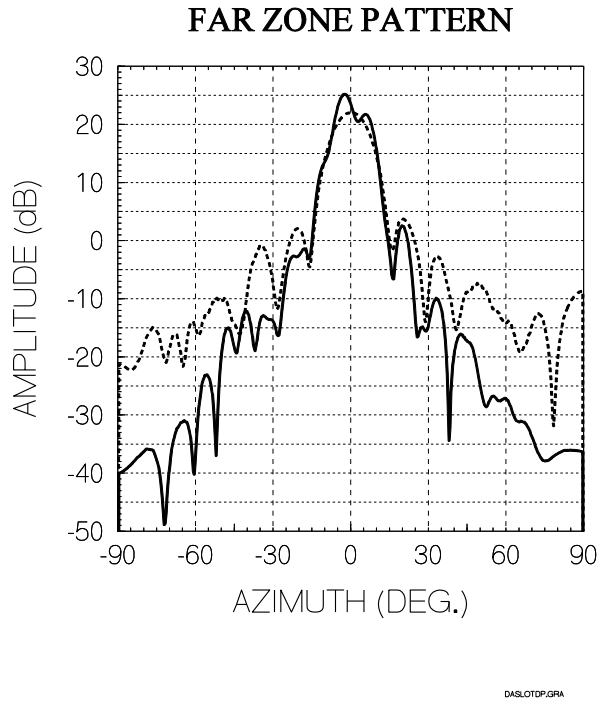

Figure 8. Measurement of the slot array using the dual probe (solid). Probe corrected measurement of the slot array using an open ended waveguide probe(dashed).

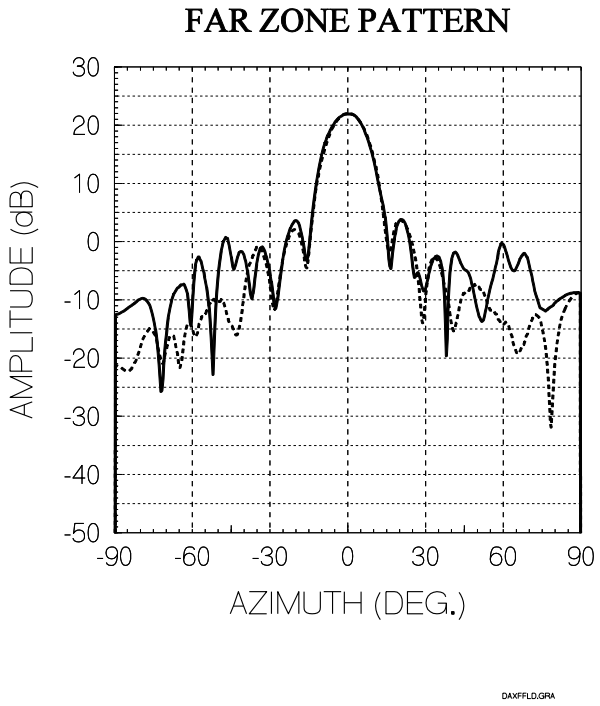

Figure 9. EPIC corrected pattern of the slot array (solid) and directly measured pattern of the slot array (dashed).

Figure 9 is the EPIC corrected version of the contaminated pattern of Figure 8. Also shown in dashed lines is the pattern of the AUT measured using near field scan of a fixed open ended waveguide probe and transforming to the far zone in the usual manner and applying probe correction to provide a reference pattern. Note that the corrected pattern and the reference pattern are in excellent agreement from -35 to +35 degrees of azimuth. The reason that this angular range is thus limited is a dynamic range issue in the measurement. To understand this we note that over the ±35 degree range the pattern of the extended probe spans 17 dB as shown in Figure 7. Thus, correction for this extended probe compresses the dynamic range of the raw measurement by 17 dB to first order. The desired corrected pattern spans 33 dB in this range of azimuth. Thus, to first order, to obtain the corrected pattern over the same range of azimuth requires a raw measurement with a dynamic range of 50 dB. A more careful analysis including the error levels in the calibration measurement and the characterization of the calibration antenna adds 5 dB to this estimate leading to a 55 dB dynamic range requirement which is just about the range available with our equipment.

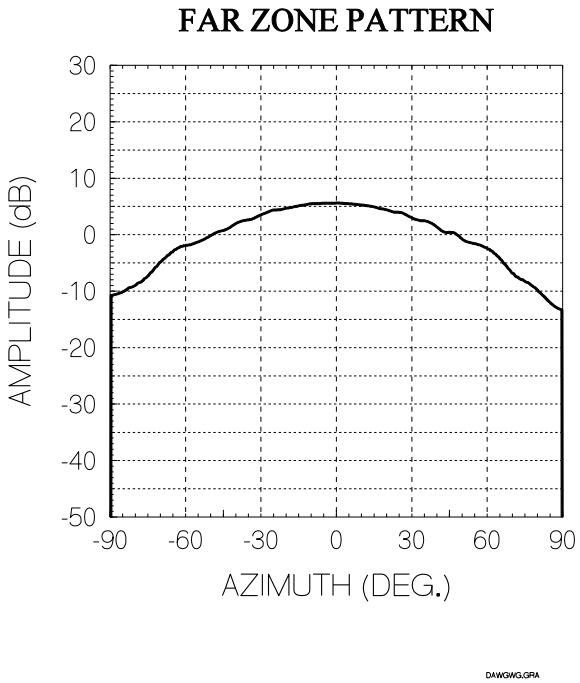

Figure 10. Measured pattern of the open ended waveguide probe.

Next we illustrate a technique by which one may extend the angular range of such an EPIC correction by more effectively using the probe. Suppose we wish to focus attention on the left side of the azimuth cut in the above example. We merely rotate the probe to place its pattern maximum on the left side of the AUT say, at -45 degrees. This arrangement is diagrammed in Figure 11. The result of the extended probe calibration measurement corresponding to Figure 7 is shown in Figure 12.

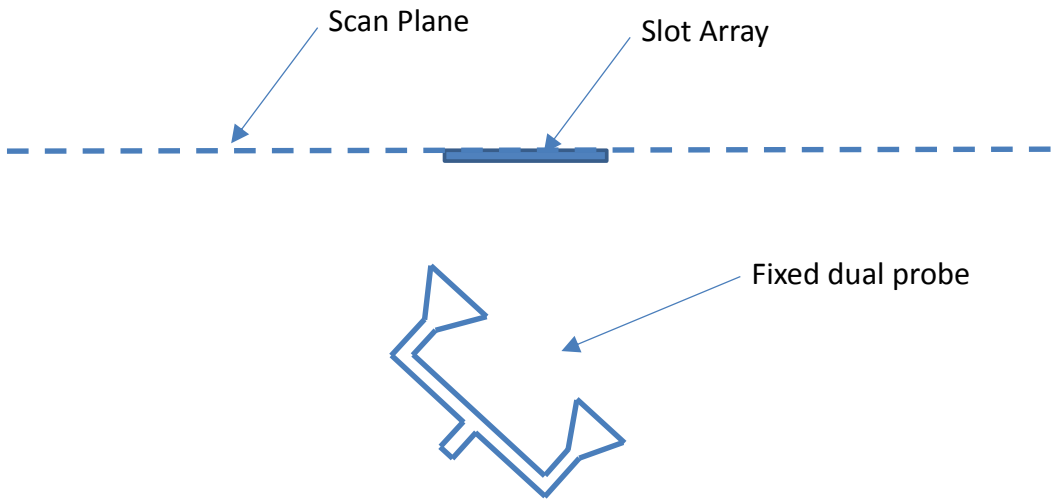

Figure11. Modified extended probe geometry.

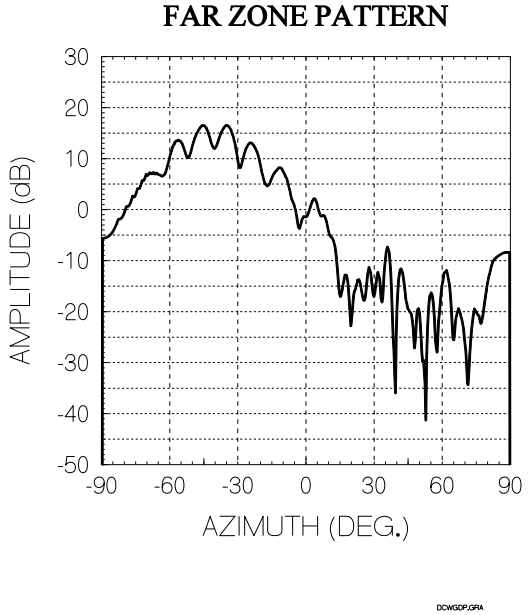

Figure 12. Extended probe calibration measurement for the geometry of Figure 11.

Figure 13 shows the result of un-calibrated measurement of the AUT using the extended probe at -45 degrees of azimuth (solid) together with the expected AUT pattern (dashed). Note that the EPIC correction now involves a reduction of the measurement amplitude rather than an increase as in typical probe correction. The result of this correction is shown in Figure 14 (solid) along with the expected result (dashed). The range of agreement is now about -45 to -10 degrees of azimuth. Thus, we have extended the azimuthal range of the result in Figure 9 by 10 degrees. Errors due to dynamic range effects are evident on the right side of the corrected pattern. Although we have not verified it experimentally, we believe that the extension could exceed the -45 degree limit on the left, perhaps extending as far as -75 degrees, were it not for the truncation error in the near field scan due to improper centering of the scan plane relative to the extended probe pointing. Evidence of this truncation effect is visible as ripple at the extreme left side of Figure 12. Note that it is the pointing of the main lobe of the extended probe that is important here whereas the ripples due to the multipath play the same role as in the earlier example.

In everyday use, planar EPIC is no more complex than ordinary probe correction. To show this, we introduce an artifact in a simple 9.3 GHz planar measurement of an X-band Narda horn in the form of a metal folding chair as shown in Figure 15a. For the calibration antenna we use an open ended waveguide for which the far zone pattern is of course known. The probe is an open ended waveguide of fixed position. The process can be summarized using the following simple formalism. We define *P(Narda)* to be the far zone pattern of the Narda horn and *P(OEWG)* to be the known pattern of the calibration antenna. *P(Meas)* is the far zone pattern resulting from transformation of the scan of the Narda horn using the fixed open ended waveguide in the presence of the chair while P(Cal) is the far zone pattern resulting from transformation of the scan of the calibration antenna (OEWG) in the presence of the chair. Finally, let *P(Ext)* be the (unknown) far zone pattern of the "extended probe;" that is the fixed probe in the presence of the chair.

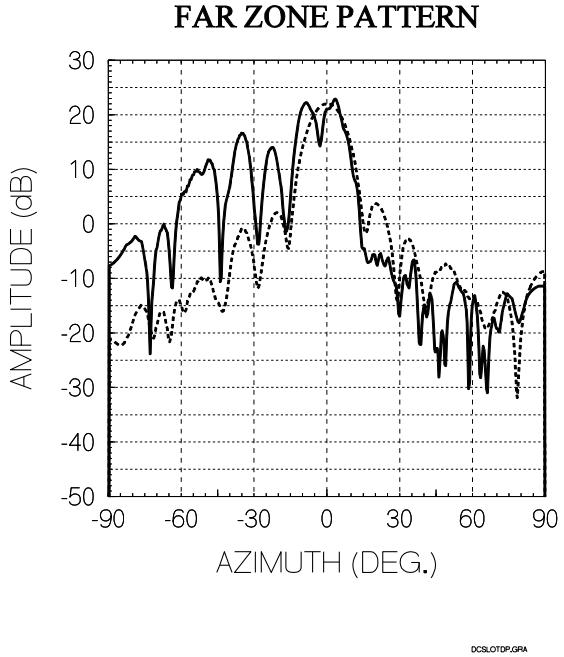

Figure 13. Uncalibrated measurement of the AUT using the extended probe at -45 degrees (solid) and the expected AUT pattern (dashed).

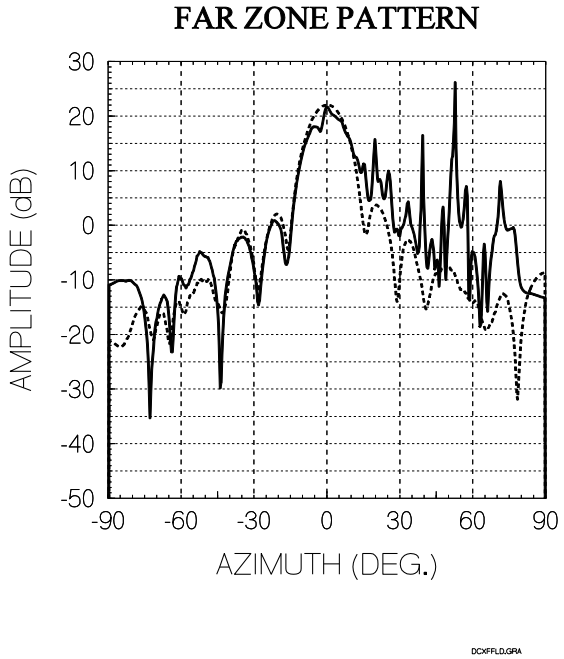

Figure 14. EPIC corrected AUT pattern (solid) and expected AUT pattern (dashed).

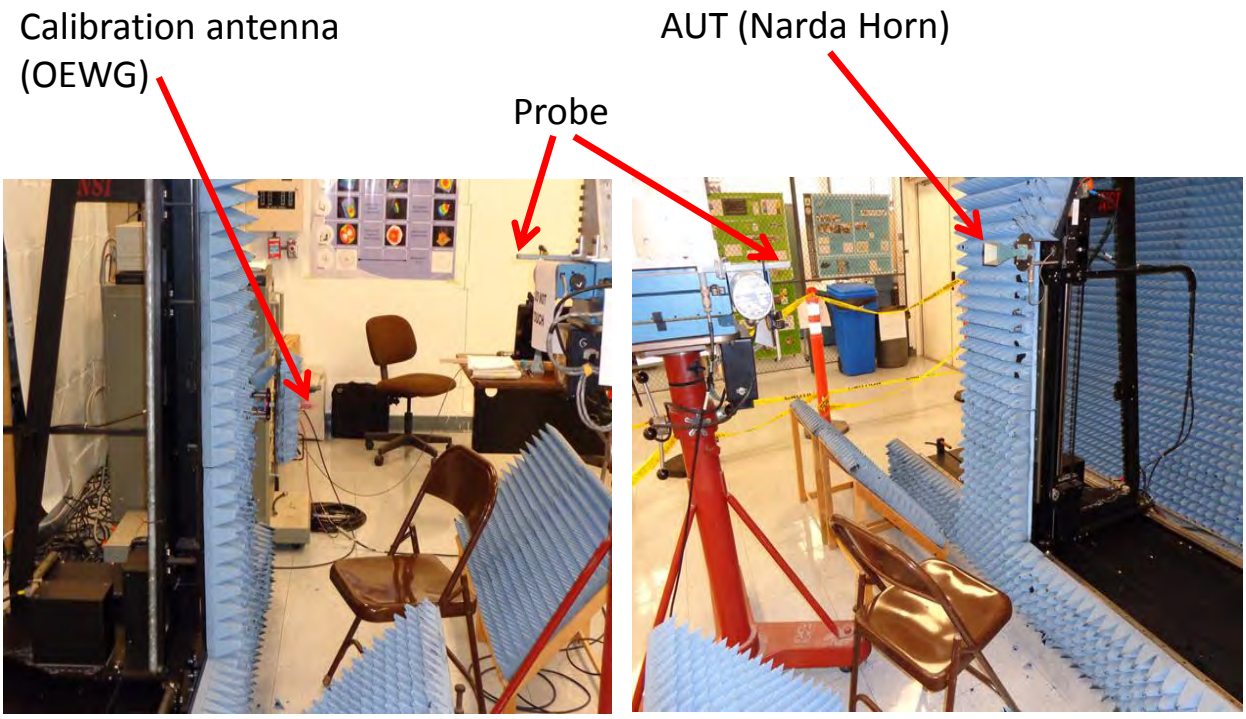

Calibration with open ended waveguide.

Measurement of Narda horn AUT.

Figure 15a. Measurements with metal chair artifact.

Fa

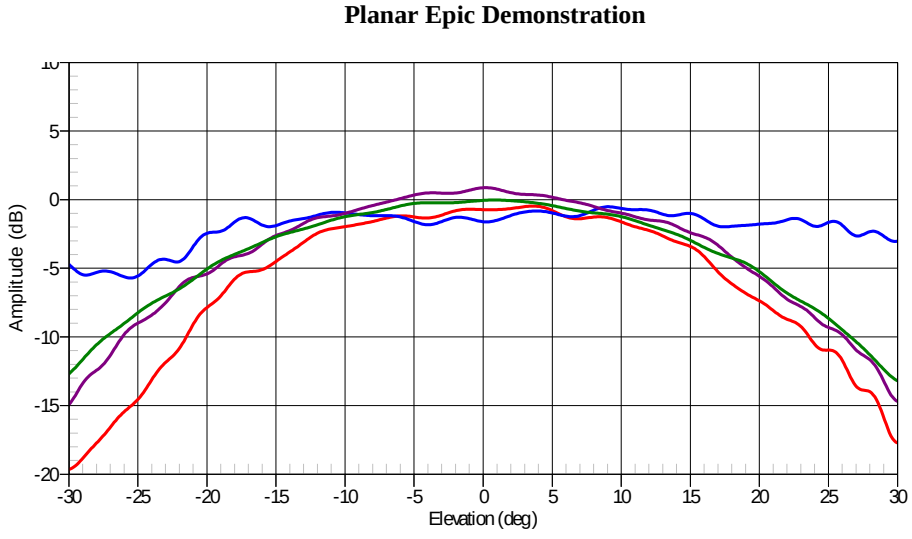

Red: Measured Pattern
Blue: Calibration Measurement

Purple: EPIC-Corrected Pattern
Green: Reference Pattern

Figure 15b. NSI 2000 Software Implementation of EPIC applied to Narda horn measurement in the presence of a metal chair.

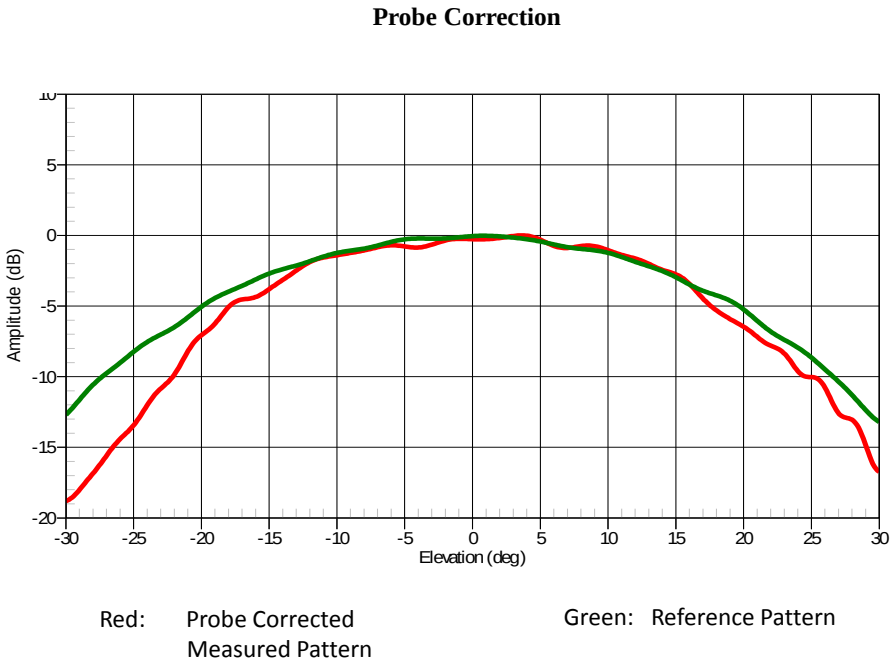

Figure 15c. Ordinary probe correction of Narda horn measurement in the presence of a metal chair.

Now, *P(Meas)*, *P(Cal)*, and *P(OEWG)* are known and we wish to obtain *P(Narda)*. Using this notation, we have,

$$P(Meas) = P(Narda) \times P(Ext)$$

$$P(Cal) = P(OEWG) \times P(Ext)$$

Since *P(Ext)* is unknown, we eliminate it and obtain,

$$P(Narda) = \frac{P(Meas)}{[P(Cal)/P(OEWG)]}$$

Written in this form we see that we merely need to divide the un-probe-corrected far zone pattern of the horn measured with the artifact present by the probe corrected far zone pattern of the calibration antenna measured with the artifact present. These two patterns are easily obtained using the planar scanner under control of the NSI 2000 software and we have used the scripting language of that software to establish a toolbar button that performs the division. The results

obtained and plotted using the NSI 2000 software are shown in Figure 15b where *P(Narda)* measured without the artifact is shown in green, *P(Meas)* is shown in red, *P(Cal)/P(OEWG)* is shown in blue, and the quotient is shown in purple. We see that EPIC has corrected the red curve to give the purple curve which is closer to the green curve taken to be the desired result. The error is no more than 1 dB over most of the 60 degree angular range. (Note that EPIC also treats the small error due to the support structure holding the fixed probe.) The traditional rule of thumb indicates that the scan geometry should yield good results from -45 to 45 degrees but scan plane truncation introduces significant ripple due to the low gain of these antennas. Therefore, we used a cosine squared taper on the raw data limiting the far zone to about -30 to 30 degrees but greatly reducing the ripple.

Finally, we have applied ordinary probe correction to *P(Meas)* to illustrate that such correction does not compensate for artifacts. The result is shown in Figure 15c where the probe corrected *P(Meas)* in red is compared with the reference pattern in green. The curves have been normalized to the plot maximum. Note that, as one might expect, the corrected curve is nowhere near as close to the reference pattern as was the purple EPIC corrected curve, even with the renormalization..

Demonstration of the Super Iso-filter

One of the most commonly applied post-measurement processing techniques in near-field antenna measurement practice is modal filtering. In spherical measurement geometry, one collects data over a near-field sphere surrounding the antenna and expands this field in vector spherical modes about a suitably chosen origin, usually the center of rotation of the positioner or the phase center of the antenna. Then one low pass filters this modal spectrum keeping only modes of order less than a maximum roughly equal to the circumference in wavelengths of the minimum size sphere enclosing the antenna. The reasoning behind this is that a radiating structure of a given size cannot efficiently radiate modes of order higher than this maximum. Thus, any higher order modes obtained in expanding the measured data must be due to artifacts lying outside the minimum size sphere enclosing the antenna and are therefore extraneous and should be filtered out. The crucial aspect of the situation that is omitted from this logic is the fact that artifacts outside the minimum sphere not only produce higher order modes, they also produce low order modes that contaminate the desired low order spectrum of the antenna under test and this cannot be remedied by simple filtering.

An application of modal filtering was recently described by Hess [8] wherein one wishes to separate the radiation from two portions of a radiating structure using only a measurement of the structure as a whole. Of the two portions of the structure one or both may be active. The inactive portion if any behaves as a passive scatterer. The approach described by Hess, dubbed the "IsoFilter™," is a straightforward application of modal filtering. One centers the spherical

expansion on the selected portion of the radiating structure and low pass filters the modal spectrum based on the minimum size sphere enclosing that portion. Recognizing that this does not rigorously separate the desired radiation, Pogorzelski [1] proposed an iterative procedure that rigorously achieves the desired decomposition. He demonstrated this computationally by separating the feed radiation from the total radiation of a reflector antenna where the reflector functions as a passive scatterer. Here we proposed to demonstrate this separation scheme using experimentally derived data.

In implementing the proposed demonstration, we selected two S-band antennas, a circularly polarized four element patch array and a linearly polarized standard gain horn. These were mounted on the roll over azimuth positioner in our tapered chamber using an appropriate fixture as shown in Figure 16. The dimensions are shown in the top view diagrammed in Figure 17.

The chamber is outfitted with an HP 8752C Network Analyzer and the MI Technologies MI-4190 Position Controller System controlled by a PC running the MI-3000 Measurement System Software Version 3.2.1, September 14, 2005. A Mini-Circuits ZRL-2400LN Low Noise Amplifier was used to partially compensate for the space loss.

A spherical scan using an open ended waveguide probe was carried out at 2.05 GHz consisting of 65 azimuth cuts equally spaced from 0 to 180 degrees of roll and sampled at 1 degree intervals from -178 to 178 degrees of azimuth. The antennas were equally excited using a 3 dB splitter. Due to the electrical size of this two antenna system, this was a near-field measurement at a probe distance of 34 feet. We transformed the measurement to the far field via the usual transformation algorithm and then applied the iterative algorithm described in [1].

The far zone fields of each antenna alone are shown in Figures 18 and 19. Figure 18 shows the principal and cross polarized patterns of the horn with the E-plane cuts on the left and H-plane cuts on the right. Figure 19 shows the corresponding patterns for the patch array alone. Note that, as expected of a circularly polarized antenna, the magnitudes of the two components of linear polarization are equal at boresight. The measured total field transformed to the far zone is shown in Figure 20 where the left plot is a cut in the E-plane of the horn showing both principal and cross polarized components while the right plot is a cut in the H-plane of the horn again showing principal and cross polarized components. Significant interference between the two antenna patterns is evident as ripple in the patterns. Upon separating the patterns of the horn and the patch array we do not expect to obtain the patterns of Figures 18 and 19 because of the mutual coupling between the antennas. What we do expect is that the separated patterns will be those of the horn plus currents induced on the horn by the patch array on the one hand and of the patch array plus the currents induced on the patch array by the horn on the other. Note that this is true *to all orders* in the multiple reflections between these antennas. The nature of these composite patterns is not known a priori so one cannot know the accuracy by inspection. Thus, we do not display all of the results here. Rather we display a particular pair of results that highlight the difference between the IsoFilter™ and the iterative technique of [1]

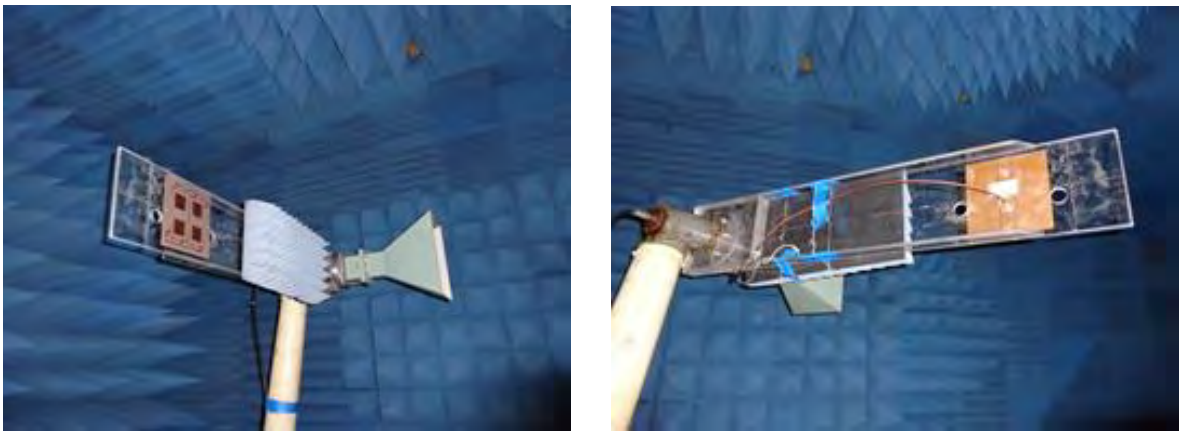

Figure 16. Two views of the two antennas with the fixture mounted on the roll over azimuth positioner at the zero degree roll position.

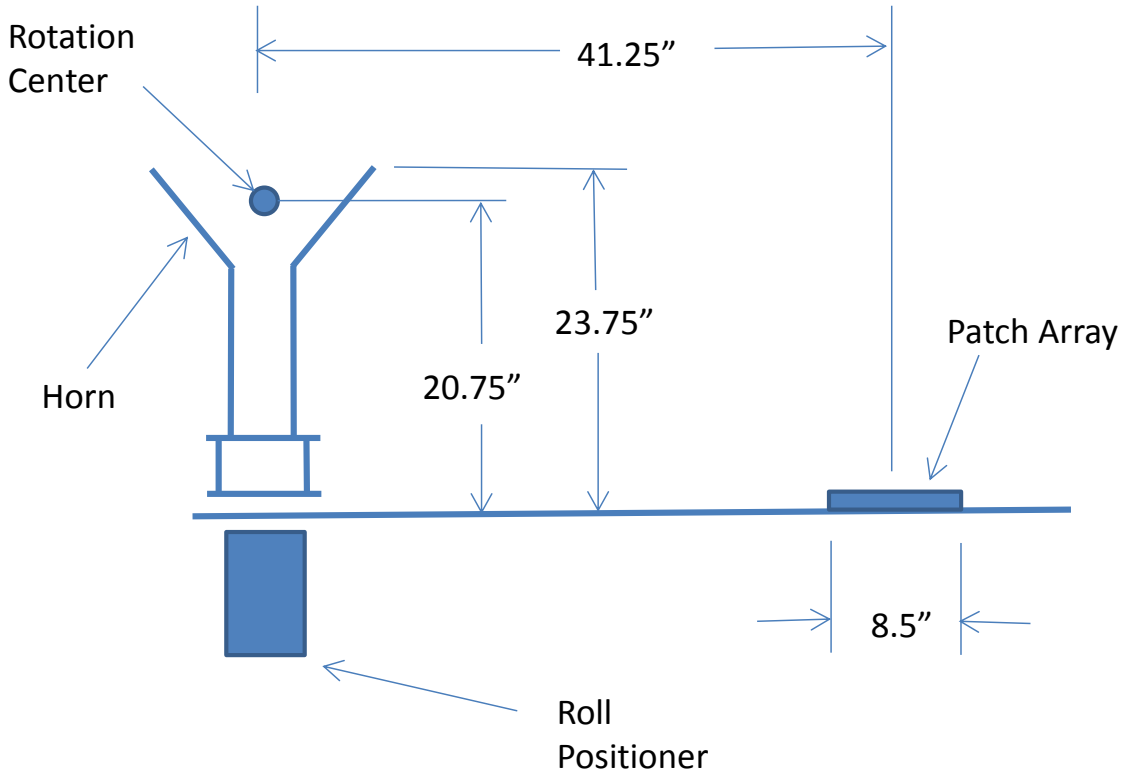

Figure 17. Top view diagram of the two antenna arrangement.

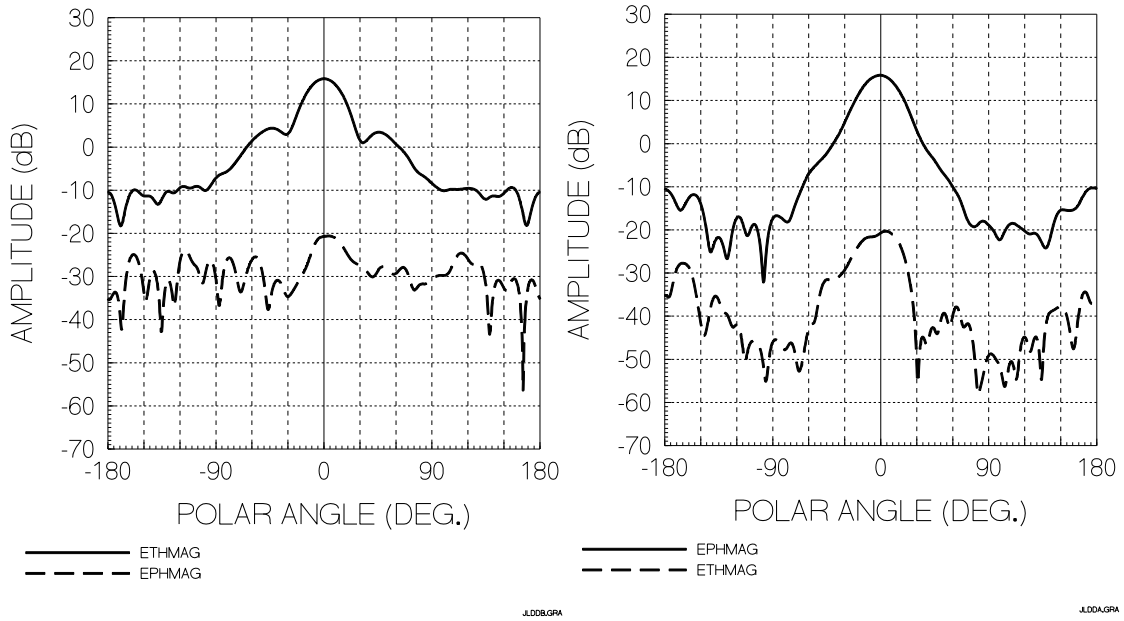

Figure 18. Principal and cross polarized far zone pattern cuts for the horn; E-plane on the left and H-plane on the right.

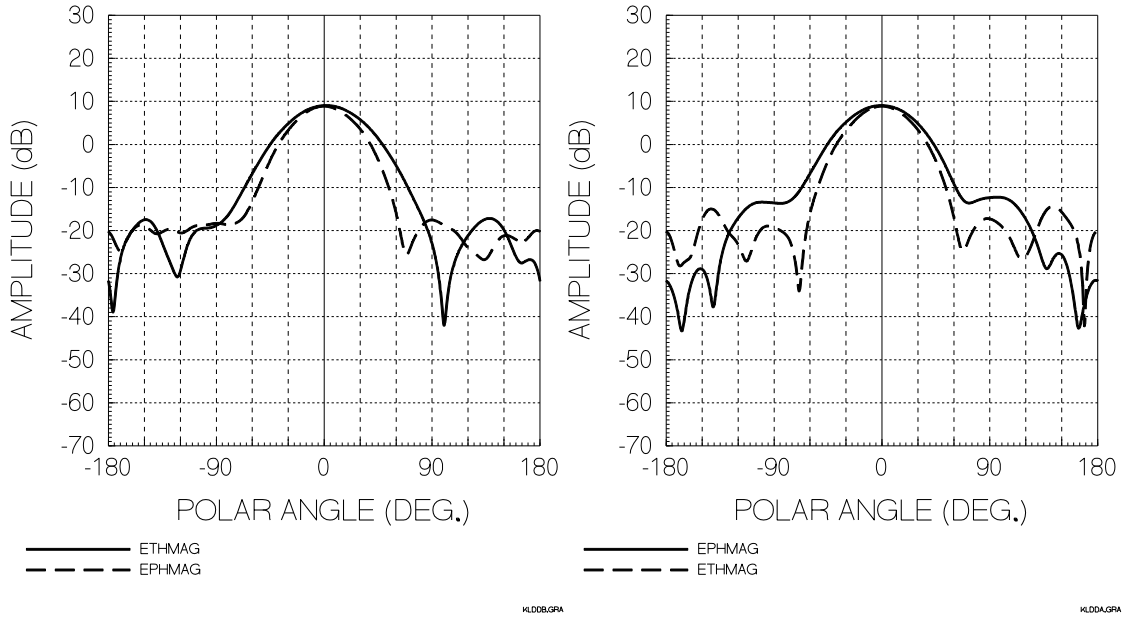

Figure 19. Principal and cross polarized far zone pattern cuts for the patch array; E-plane on the left and H-plane on the right.

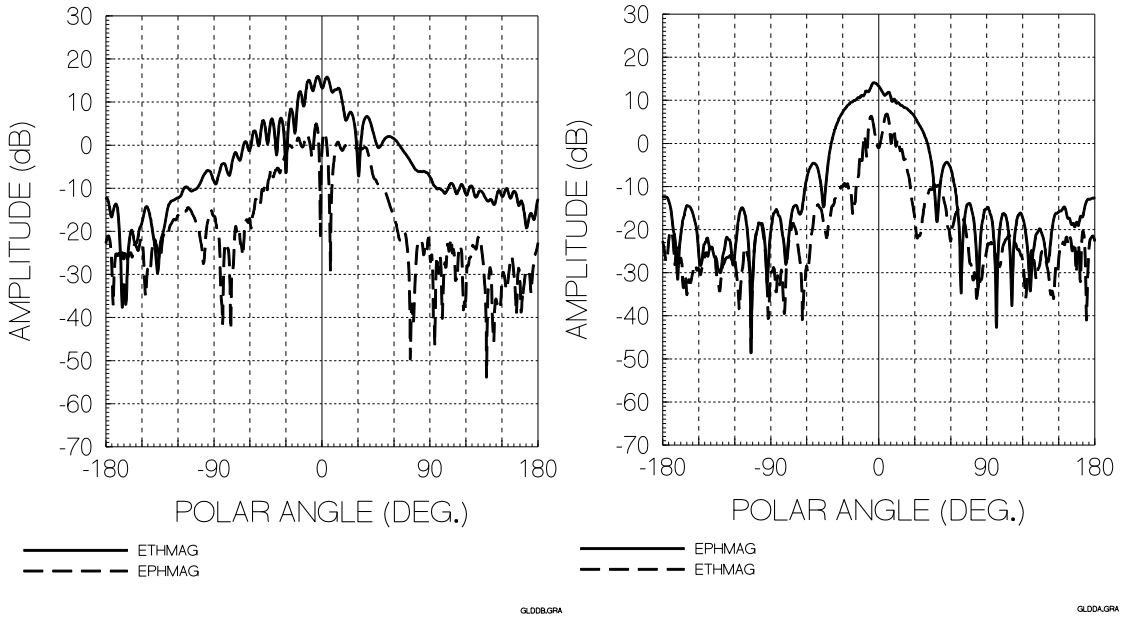

Figure 20. Principal and cross polarized far zone pattern cuts for the two antennas; E-plane on the left and H-plane on the right.

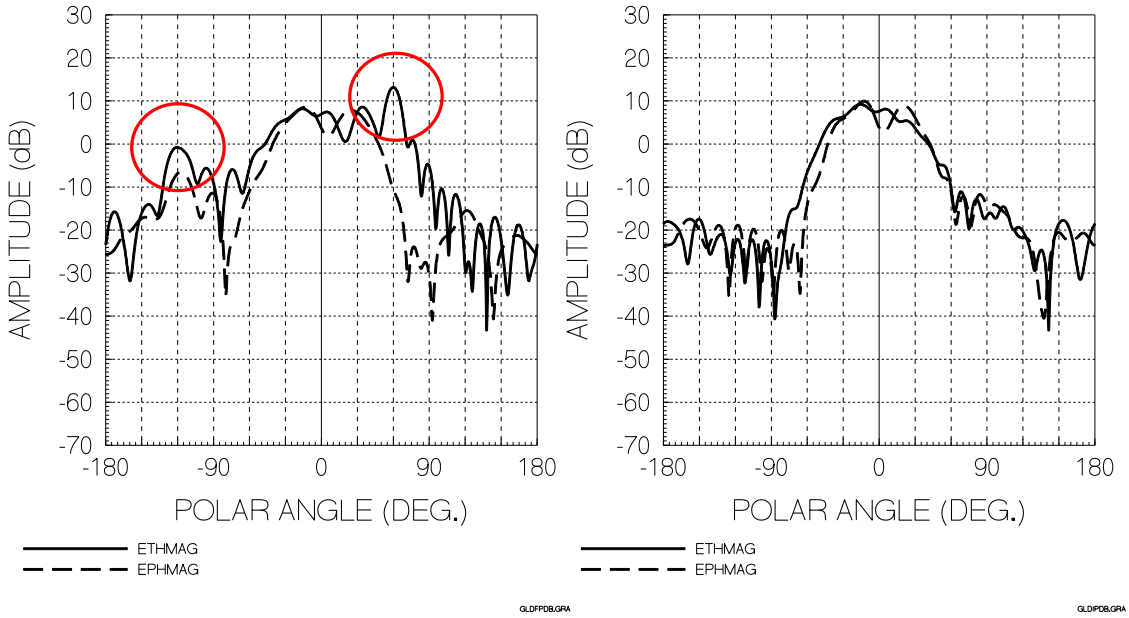

Figure 21. E-plane patterns of the patch array obtained via the IsoFilter™ on the left and iteration on the right.

Figure 21 shows two selected E-plane patterns that illustrate the difference we wish to point out. The patterns on the left are obtained from the fields of Figure 20 by centering a modal expansion on the patch array and filtering to 16 polar modes to produce the IsoFilter™ result. The patterns on the right were obtained by applying the iterative algorithm. Note that in the IsoFilter™ result there are two lobes (circled in red) that do not appear in the iteration result, one at -120 degrees and one at +60 degrees. These are the angles where the horn and the patch array are approximately in line with the radius vector to the probe. We contend that these represent IsoFilter™ error due to improper treatment of the interaction between the antennas. We endeavor to support this contention via a measurement with only the patch array excited. We expect that in such a case, to first order in multiple reflections, the IsoFilter™ will no longer produce the erroneous lobes. Also to first order, the iterative approach will produce the field of the patch array alone and, separate from it, the field of the currents induced on the horn by the patch array. The results corresponding to those in Figure 21 are shown in Figure 22. These represent the radiation from the patch array with currents modified by the presence of the unexcited horn. Note that the IsoFilter™ results on the left do not have the lobes circled in red in Figure 21 and, of course, neither do the iteration results on the right.

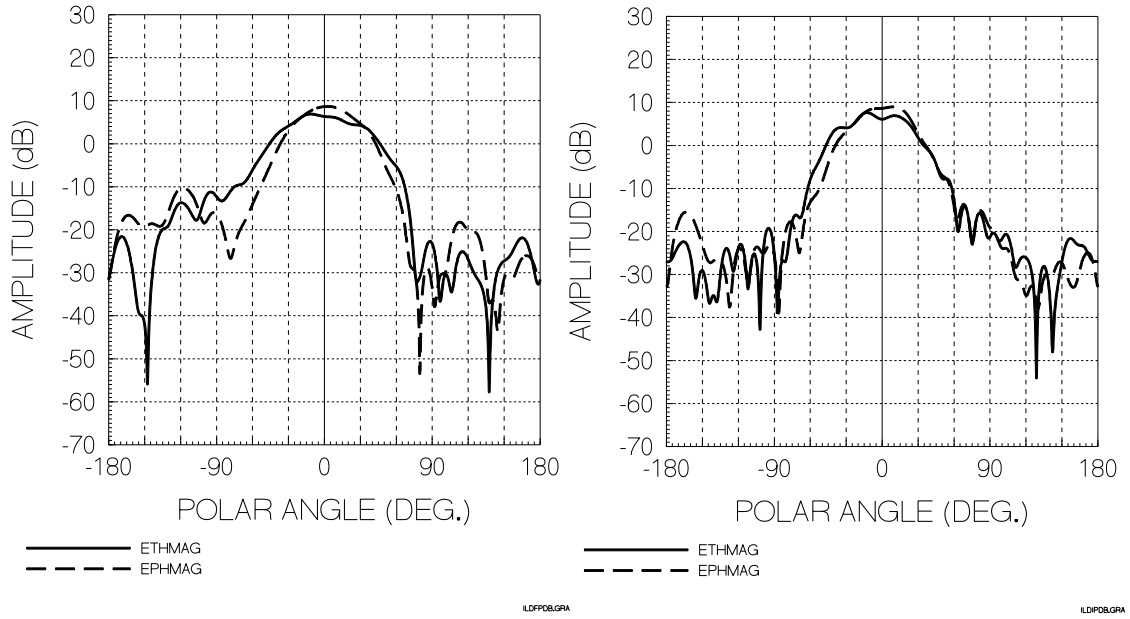

Figure 22. E-plane patterns of the patch array obtained via the IsoFilter™ on the left and iteration on the right when the horn is not excited.

The error identified in Figure 21 occurs because, in the spherical expansion of the fields about an origin centered on the patch array, the portion of the field originating at the horn is nonsingular and thus should be represented by a series of spherical Bessel functions, that is, half incoming

and half outgoing waves, and this part of the field eliminated from the expansion. In the IsoFilter™ process however, this field is included and taken to be entirely outgoing leading to the erroneous lobes. These lobes do not significantly appear if the horn is not excited because, to first order in the multiple reflections, the Bessel terms are absent from the field expansion about the patch array. A similar error occurs for similar reasons when one applies the IsoFilter™ to obtain the radiation from the currents induced on the horn when the patch array only is excited. These results are shown on Figure 23 where the plots are normalized to the directivity of the patch array; that is, the normalization is the same as that of the plots for the patch array pattern normalized to directivity.

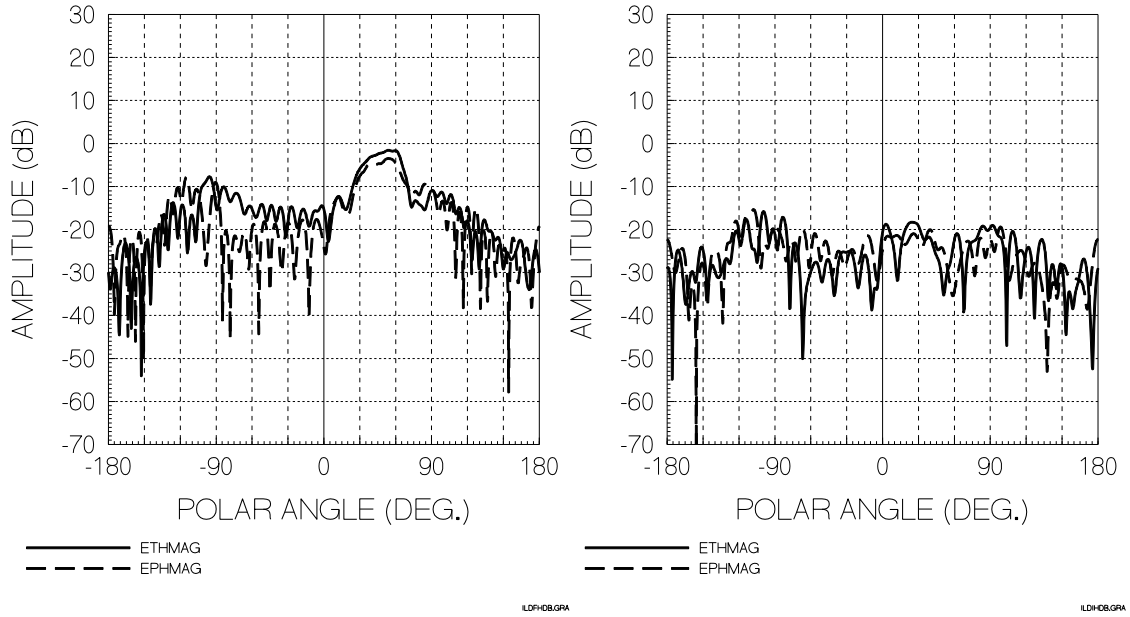

Figure 23. E-plane patterns of the horn scattering obtained via the IsoFilter™ on the left and iteration on the right when the horn is not excited.

A final test was performed with the horn physically removed from the fixture. In this case of course no currents are induced on the horn to radiate back to the patch array and the IsoFilter™ and iteration results become essentially identical as shown in Figure 24. We believe that the differences between Figure 24 and Figure 19 are due to chamber effects; i.e., fixturing, wall reflections, and positioner inaccuracies.

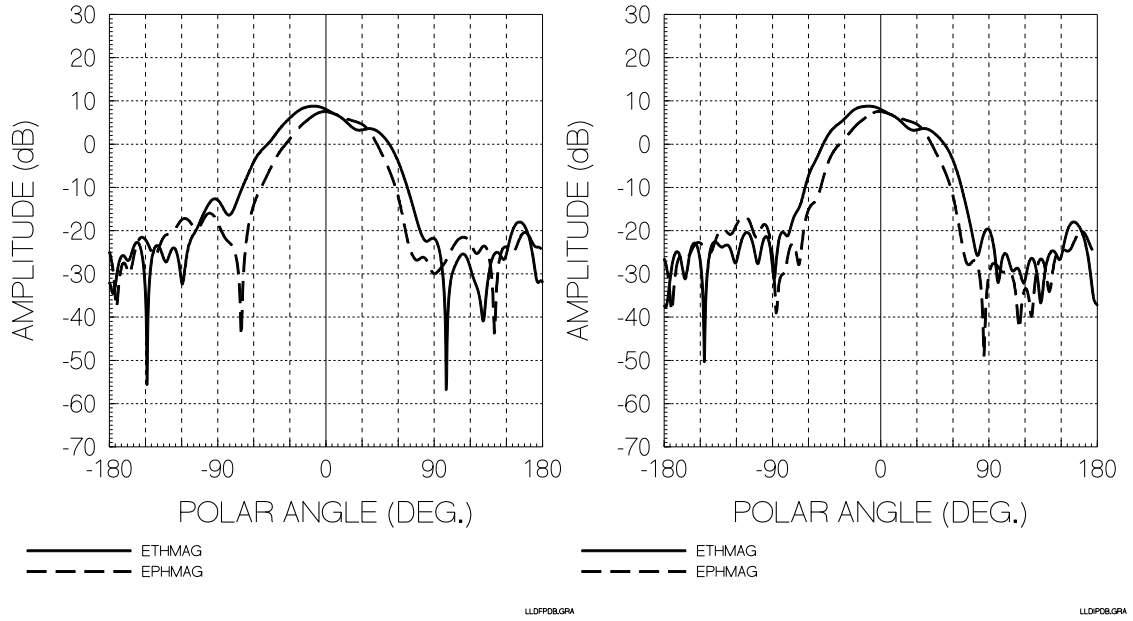

Figure 24. E-plane patterns of the patch array obtained via the IsoFilter™ on the left and iteration on the right with the horn absent.

General Discussion of Results

In the process of achieving each of the objectives described above we have shown that the basic concepts are valid and that each has limitations that must be understood in order to use them effectively. Moreover, there are questions that remain unanswered concerning the behavior of the algorithms involved.

In the case of the extrapolation of the measurement plane in planar nearfield scanning, one cannot expect to extrapolate an arbitrarily small scan plane to infinite size. One must sample a substantial region and can then extrapolate to a limited degree which may in many cases result in the desired full hemispherical far zone pattern. As mentioned earlier, it will be important to establish rules of thumb for the required scan plane electrical size versus antenna gain and appropriate aperture truncation. This will probably require detailed stationary phase analysis of the transform integral.

Extended Probe Instrument Calibration (EPIC) has been demonstrated in planar scanning first under rather contrived conditions and then in a more realistic scenario. We have shown that the truncation of the measurement plane produces extraneous ripple due to the wide beams of the probe and calibration antennas and we have mitigated this via measurement plane tapering as is commonly done. The results obtained using the new toolbar button in the NSI software show

reduction but not elimination of the error due to the artifact on the range. This should be further investigated to determine the attainable accuracy. Furthermore, there are clearly limitations as to the allowable locations of artifacts as determined by the equivalence principle and these should be studied and delineated to guide future use of this concept. A related approach is the use of the far zone field to obtain a spherical mode expansion representing the radiated field. This permits the use of mode filtering with its own set of equivalence principle based limitations. These too should be studied.

The iterative filtering algorithm has been shown to work well for the example chosen but, here again there are generalizations to be pursued and limitations to be understood. In particular, the treatment of more than two expansion centers is of interest. There is also the question of how close the centers can be placed and still permit accurate decomposition of the field and robust convergence in a reasonable number of iterations. Additionally, one might identify the currents induced on one antenna by radiation from the other one and thus study mutual coupling.

We have achieved the original objectives of the project and then some. There remain opportunities for further development of the techniques and further investigation of their properties as discussed above. As the techniques are matured in this manner, we intend to submit detailed descriptions of the various aspects of the work for publication in peer reviewed archival journals. We further intend to pursue opportunities for transitioning these methods to industry where they can provide opportunities for better understanding of the performance of antennas for practical application.

Concluding Remarks

This has been an extremely interesting short term innovative research (SBIR) activity. The results are all promising to varying degree and represent tools of great utility in understanding antenna pattern measurements both near field and far field. We are most interested in continuing our investigations in this area as outlined above as well as providing research opportunities for students in the microwave and antenna area at CSUN. The recently upgraded NSI Planar Scanner is an important laboratory resource in this regard. While this is also true of the tapered chamber, its use on the present project revealed a number of deficiencies that require attention if it is to be a viable teaching tool. We are taking the first step in this by refurbishing the mounting for the open ended waveguide probe. This will greatly facilitate alignment. We have also noted a ±1 degree backlash in the roll positioner. This may require replacement. Finally, the chamber system is currently limited to a frequency range of 1 to 3 GHz primarily due to rf equipment limitations. Our long range goal is to completely replace the rf electronics thus extending the frequency range up to at least 20 and perhaps 30 GHz. Another goal is the addition of a roll over azimuth positioner to the planar scanner to permit spherical scanning as well. Such flexibility would be a very valuable teaching tool permitting treatment of all three common canonical scan

surfaces. The resources for all these goals have yet to be identified. Nevertheless, in the short term, the present systems with proper maintenance and a few minor upgrades will permit teaching and research within limits with significant associated benefit to military, industrial, and academic practitioners involved in antenna performance assessment.

References

1. R. J. Pogorzelski, "An Effective Method of Isolating Portions of a Radiator in Near-field or Far-field Antenna Measurement", IEEE Antennas and Propagation Magazine, 55, 3, June 2013.

2. R. J. Pogorzelski, "Extended Probe Instrument Calibration (EPIC) for Accurate Spherical Near-field Antenna Measurements," IEEE Trans. on Antennas and Propagation, AP-57,3366-3371,October 2009.

3. R. J. Pogorzelski, "Experimental Demonstration of the Extended Probe Instrument Calibration (EPIC) Technique," IEEE Trans. on Antennas and Propagation, AP-58, 2093-2097, June 2010.

4. E. Martini, O. Breinberg, and S. Maci, "Reduction of Truncation Errors in Planar Near-Field Aperture Antenna Measurements Using the Gerchberg-Papoulis Algorithm," IEEE Trans. on Antennas and Propagation, AP-56, 3485-3493, November 2008.

5. R. W. Gerchberg, "Super-resolution through Error Energy Reduction," Optica Acta, Vol. 21, No. 9, 709-720, 1974.

6. A. Papoulis, "A New Algorithm in Spectral Analysis and Band-Limited Extrapolation," IEEE Trans. Circuits and Systems, CAS-22, 735-742, September 1975.

7. S. Rengarajan and R. J. Pogorzelski, "On the Gerchberg-Papoulis Algorithm for Extrapolating Antenna Patterns," IEEE AP-S / URSI International Symposium, Memphis, TN, July 2014.

8. D. W. Hess, "The IsoFilter™ Technique: A Method of Isolating the Pattern of an Individual Radiator from Data Measured in a Contaminated Environment," IEEE Antennas and Propagation Magazine, 52, 174-181, Feb. 2010.